Journal of Anatomy

J. Anat. (2019) **234**, pp679–693 doi: 10.1111/joa.12957

Trabecular architecture of the great ape and human femoral head

Leoni Georgiou,[1] Tracy L. Kivell,[1,2] Dieter H. Pahr,[3,4] Laura T. Buck[5] and Matthew M. Skinner[1,2]

[1]*Skeletal Biology Research Centre, School of Anthropology and Conservation, University of Kent, Canterbury, UK*
[2]*Department of Human Evolution, Max Planck Institute for Evolutionary Anthropology, Leipzig, Germany*
[3]*Institute for Lightweight Design and Structural Biomechanics, Vienna University of Technology, Vienna, Austria*
[4]*Department of Anatomy and Biomechanics, Karl Landsteiner Private University of Health Sciences, Krems an der Donau, Austria*
[5]*Department of Anthropology, University of California, Davis, CA, USA*

Abstract

Studies of femoral trabecular structure have shown that the orientation and volume of bone are associated with variation in loading and could be informative about individual joint positioning during locomotion. In this study, we analyse for the first time trabecular bone patterns throughout the femoral head using a whole-epiphysis approach to investigate how potential trabecular variation in humans and great apes relates to differences in locomotor modes. Trabecular architecture was analysed using microCT scans of *Pan troglodytes* (n = 20), *Gorilla gorilla* (n = 14), *Pongo* sp. (n = 5) and *Homo sapiens* (n = 12) in MEDTOOL 4.1. Our results revealed differences in bone volume fraction (BV/TV) distribution patterns, as well as overall trabecular parameters of the femoral head between great apes and humans. *Pan* and *Gorilla* showed two regions of high BV/TV in the femoral head, consistent with hip posture and loading during two discrete locomotor modes: knuckle-walking and climbing. Most *Pongo* specimens also displayed two regions of high BV/TV, but these regions were less discrete and there was more variability across the sample. In contrast, *Homo* showed only one main region of high BV/TV in the femoral head and had the lowest BV/TV, as well as the most anisotropic trabeculae. The *Homo* trabecular structure is consistent with stereotypical loading with a more extended hip compared with great apes, which is characteristic of modern human bipedalism. Our results suggest that holistic evaluations of femoral head trabecular architecture can reveal previously undetected patterns linked to locomotor behaviour in extant apes and can provide further insight into hip joint loading in fossil hominins and other primates.

Key words: African apes; cancellous bone; functional morphology; *Gorilla*; hominid; *Pan*; *Pongo*.

Introduction

The morphology of the proximal femur has played a key role in the reconstruction of locomotion in extant and extinct primates (e.g. McHenry & Corruccini, 1978; Burr et al. 1982; Ruff et al. 1991; Ruff & Runestad, 1992; Ruff, 1995; Harmon, 2007, 2009a; Ruff & Higgins, 2013) and particularly in understanding the form of bipedalism used by australopiths (Stern & Susman, 1983; Susman et al. 1984; Crompton et al. 1998; Carey & Crompton, 2005; Harmon, 2009b; Lovejoy & McCollum, 2010; Raichlen et al. 2010; DeSilva et al. 2013). External morphology provides considerable evidence of functional links between morphology and locomotion. However, due to possible phylogenetic lag, which results in traits that are no longer functionally significant being present, inferences about behaviour based on external traits alone have been questioned (e.g. Ward, 2002). Variation in internal trabecular (or cancellous) bone structure across different regions of the skeleton can provide additional evidence to help reconstruct joint postures and to infer potential differences in locomotor behaviour in extant and extinct primates (e.g. Thomason, 1985a,b; Ryan & Ketcham, 2002; Volpato et al. 2008; Ryan & Shaw, 2012; Tsegai et al. 2013; Skinner et al. 2015; Stephens et al. 2016). Indeed, the ability of trabecular bone to reflect mechanical loading was first noted in the human proximal femur (Ward, 1838; Wolff, 1870; Wolff, 1892). It is not yet fully understood how mechanical or non-mechanical factors trigger and ultimately affect the organisation of trabeculae. For example, a range of activities, including high strain/low frequency loading and low strain/high frequency loading have been shown to elicit trabecular reorganisation (Rubin et al. 1990, 2001; Judex et al. 2003; Wallace et al. 2014).

Correspondence
Leoni Georgiou, School of Anthropology and Conservation, Marlowe Building, University of Kent, Canterbury, Kent CT2 7NR, UK.
E: lg400@kent.ac.uk

Accepted for publication *16 January 2019*
Article published online *21 February 2019*

Furthermore, differences in body mass (Scherf, 2008; Cotter et al. 2009; Doube et al. 2011; Fajardo et al. 2013; Ryan & Shaw, 2013), hormones (e.g. Gunness-Hey & Hock, 1984; Miyakoshi, 2004; Walsh, 2015) and genetic or systemic factors (Havill et al. 2010; Tsegai et al. 2018) have been shown to influence aspects of trabecular structure as well. However, computational (e.g. Huiskes et al. 2000; Keaveny et al. 2001) and experimental studies have demonstrated that modelling of trabeculae is correlated with applied loads, and trabecular strut reorganisation can be instigated by changes in the direction, magnitude or frequency of load (Biewener et al. 1996; Mittra et al. 2005; Pontzer et al. 2006; Polk et al. 2008; Barak et al. 2011). Furthermore, trabecular bone volume fraction (BV/TV) and trabecular strut alignment (degree of anisotropy, or DA) explain up to 98% of bone stiffness (i.e. Young's modulus of elasticity; Odgaard, 1997; Stauber et al. 2006; Maquer et al. 2015). Thus, variation in the distribution of BV/TV and DA can provide insight into joint loading and, in turn, locomotor behaviours in primates.

Several studies have revealed that variation in the trabecular architecture of the primate hip and proximal femur is associated with differences in locomotion (e.g. Rafferty & Ruff, 1994; MacLatchy & Müller, 2002; Volpato et al. 2008; Ryan & Shaw, 2012; Saers et al. 2016). For example, Volpato et al. (2008) demonstrated that the orientation of trabecular struts in the ilium and femoral neck is associated with joint positioning in the hip of bipedally trained Japanese macaques and reflects alterations in the direction of load. Comparable changes in trabecular structure that reflect differences in joint orientation were also found in the distal femora of guinea fowls (Pontzer et al. 2006) and distal tibiae of sheep (Barak et al. 2011). Furthermore, Scherf (2008) found that trabecular structure within the femoral head, neck and both trochanters of climbing primates (e.g. *Alouatta seniculus*) had more isotropic architecture, whereas specialised primates (e.g. *Homo sapiens*) in which the femur experienced more stereotypical loading, had more anisotropic structure. Similar results were found in leaping primates, which in comparison with non-leaping primate species, had more anisotropic trabeculae in the inferior aspect of the femoral head (Ryan & Ketcham, 2002), and a different principal strut orientation (Ryan & Ketcham, 2005).

More recently, Ryan & Shaw (2012) investigated the trabecular patterns of the femoral head in several anthropoid taxa and found that different suites of trabecular variables could distinguish among taxa and locomotor groups. In particular, modern humans were distinct in having relatively few, highly anisotropic trabeculae that are thin and plate-like, *Pan* had relatively numerous, thick and isotropic trabeculae, and *Pongo* had relatively few and isotropic trabeculae. Additional studies investigating different human samples have also shown that femoral head trabecular structure reflects variation in mobility levels, with more sedentary agriculturalists having relatively low BV/TV compared with more active foragers (Ryan & Shaw, 2015; Saers et al. 2016; Ryan et al. 2018). Interestingly, more active human foragers have relatively high BV/TV that falls within the range of most extant hominoids apart from *Pan* (Ryan et al. 2018). Despite this overlap in BV/TV between some human samples and other hominoids, humans have consistently been shown to have the most anisotropic femoral head structure compared with other great apes (Ryan & Shaw, 2015; Ryan et al. 2018). Furthermore, the human trabecular pattern has been shown to develop during ontogeny when independent bipedalism develops and the gait matures (Ryan & Krovitz, 2006; Reissis & Abel, 2012; Milovanovic et al. 2017). Altogether, these studies suggest that the trabecular bone of the femoral head holds a strong functional signal of locomotor loading in primates.

Conversely, other studies have failed to detect a strong locomotor signal in the femoral head (Ryan & Walker, 2010; Shaw & Ryan, 2012), femoral neck (Fajardo et al. 2007) and distal femur (Carlson et al. 2008). Carlson et al. (2008) did not detect differences in the DA of the distal femoral metaphysis between mice with turning locomotion and mice with non-turning locomotion. Similarly, Ryan & Walker (2010) did not find any significant differences in the DA and BV/TV patterns of the femoral head in a broad sample of platyrrhines and catarrhines. Furthermore, Shaw & Ryan (2012), who examined the subarticular trabecular and mid-diaphyseal cortical patterns in the femur and humerus of a sample of primates, concluded that only the mid-diaphyseal cortical bone contains a clear functional signal linked to the differential use of the two limbs between different locomotor groups.

The discrepancy in the findings of previous studies may, in part, be an artefact of the volume-of-interest (VOI) method that was used. A VOI quantifies only a subsample of trabecular structure within a given region, and results can vary depending on its size and position (Fajardo & Müller, 2001; Kivell et al. 2011). Additionally, challenges arise when extracting homologous VOIs in taxa that vary in external morphology. Prior research has demonstrated that additional functional insight can be gained from investigating the trabecular architecture within an epiphysis as a whole (Tsegai et al. 2013, 2018; Skinner et al. 2015; Stephens et al. 2016; Sylvester & Terhune, 2017). Here we apply a whole-epiphysis approach to study the trabecular structure throughout the femoral head of chimpanzees (*Pan troglodytes*), lowland gorillas (*Gorilla gorilla*), orangutans (*Pongo* sp.) and humans (*Homo sapiens*), which vary in locomotor behaviours and are relevant to the reconstruction of locomotion in fossil hominins.

Locomotion, hip morphology and predicted joint posture

Habitual locomotor activities and associated hip joint angles vary between great apes and humans (Fig. 1). Chimpanzees

are predominantly terrestrial/arboreal quadrupedal knuckle-walkers, but also engage frequently in arboreal climbing and, less frequently, bipedalism (Hunt, 1991; Doran, 1992; Doran, 1993a,b). In all these locomotor modes, the hindlimb plays a key role in propulsion and experiences higher vertical force than the forelimb does (Demes et al. 1994; Hanna et al. 2017). During terrestrial quadrupedalism in chimpanzees, the mean hip angle at foot touchdown is 65° and at toe-off it is 98.2° (Finestone et al. 2018). Kinematics during chimpanzee vertical climbing have, to our knowledge, only been studied in one individual and show that the flexion–extension range at the hip increases substantially compared with terrestrial quadrupedalism, with hip angles ranging from ~ 25° to ~ 105° (Nakano et al. 2006). A more comprehensive study of bonobos (n = 4 adults), which share similar hindlimb anatomy with chimpanzees (e.g. Payne et al. 2006; Myatt et al. 2011), yielded hip angles ranging from 55° to 135° during vertical climbing (Isler, 2005).

Lowland gorillas are also predominantly quadrupedal knuckle-walkers (Remis, 1995; Crompton et al. 2010). They often engage in arboreal climbing and bipedalism, but less frequently so than chimpanzees (Remis, 1995; Crompton et al. 2010). During terrestrial quadrupedalism in gorillas, hip angles range from 77° at foot touchdown to 120.6° at toe-off (Finestone et al. 2018). During vertical climbing, hip angle range is similar to that of bonobos, ranging from approximately 45° to 135° (Isler, 2005). *Gorilla* climbing frequency and technique varies with sex and body size, with the range of hip flexion-extension being reduced in larger males compared with smaller females (Remis, 1995, 1999; Isler, 2005). However, gorillas show less intraspecific variation in climbing techniques than bonobos (Isler, 2005).

Orangutans employ a complex set of locomotor behaviours, which are mostly torso orthograde, including vertical climbing, bridging, suspension from various limbs, and terrestrial quadrupedalism (Cant, 1987; Isler & Thorpe, 2003; Thorpe & Crompton, 2006; Thorpe et al. 2009). Their hips are more mobile than those of other apes, which allows them to use their hindlimbs in more varied ways (Morbeck & Zihlman, 1988; Tuttle & Cortright, 1988; Isler, 2005). During terrestrial locomotion, the orangutan hip angle is 68.3° at touchdown and 107.3° at toe-off (Finestone et al. 2018). During vertical climbing, orangutans are able to lift their feet further above their hips than African apes, such that their flexion-extension angle ranges from around 30°–135° (Isler, 2005).

Adult humans walk exclusively terrestrially on two legs, extending both their hips and knees (Alexander, 1994). During the gait cycle, hip extension reaches 160° at touchdown and 175° at toe-off (Abbass & Abdulrahman, 2014). Humans also engage in running, which alters the joint angle of the hip and the resulting load on the femoral head (Ounpuu, 1990, 1994; Van der Bogert et al. 1999; Giarmatzis et al. 2015). Increase in speed is linked to more flexed hip joints and a generally increased range of motion at the hip (Mann & Hagy, 1980; Novacheck, 1998). At touchdown during running the hip is flexed 30°–40°, while also being externally rotated, and at push off it is extended and internally rotated (Slocum & James, 1968). Furthermore, during running (3.5 m s^{-1}), loads have been shown to increase to greater than double that of walking (1.5 m s^{-1}; Van der Bogert et al. 1999).

Great apes and humans vary in the external morphology of the hip joint. Chimpanzees and gorillas have a relatively small femoral head, a short femoral neck and a superoinferiorly expanded greater trochanter as compared with orangutans (McHenry & Corruccini, 1978; Harmon, 2007). Chimpanzees have a 'laterally facing acetabulum' (Jenkins, 1972); however, comparative quantitative data of acetabulum anteversion do not exist for apes and humans (Hogervorst et al. 2009 and references therein). Furthermore, in gorillas, the acetabulum is relatively deep compared with other apes (Schultz, 1969), perhaps reducing the capacity for mobility at the hip. In orangutans, the greater trochanter is less superoinferiorly expanded than in the African apes and is positioned inferiorly to the femoral head, which

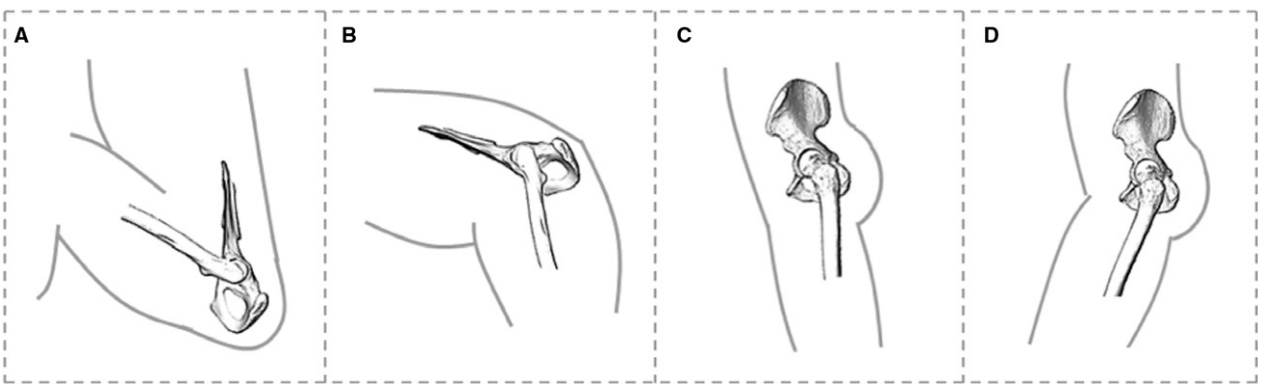

Fig. 1 Comparison of hip posture during different habitual locomotor activities in great apes (A,B) and humans (C,D). (A) Great ape hip posture in maximum hip flexion (~ 55°–60°) during climbing (Isler, 2005). (B) Great ape hip posture at toe-off (~ 110°) during terrestrial knuckle-walking (Finestone et al. 2018). (C) Human hip posture at toe-off (~175°). (D) Human hip posture at heel-strike (~160°).

may enhance rotational capacity at the hip joint (Aiello & Dean, 2002; Harmon, 2007). Orangutans also have a relatively large head, long neck and a greater trochanter that is less superoinferiorly expanded than that of African apes and which is positioned inferiorly relative to the femoral head (Aiello & Dean, 2002; Harmon, 2007). These features of the orangutan proximal femur, plus the absence of a subchondral ligamentum teres insertion at the centre of the femoral head (Crelin, 1988; Ward, 1991; Ruff, 2002; Harmon, 2007), enhance rotational capacity and allow greater mobility at the hip joint compared to other hominoids.

Humans have a long femoral neck and a valgus angle at the knee, which compensate for the mechanical disadvantage of increased bi-acetabular distance (Lovejoy, 1975; McHenry & Corruccini, 1978; Rafferty, 1998; Lovejoy et al. 2002; Harmon, 2007) and result in adduction of the hips during the stance phase (O'Neill et al. 2015). The greater trochanter is less superoinferiorly expanded compared with other apes (Harmon, 2007). Furthermore, the human acetabulum is relatively deep and the femoral head relatively large (Schultz, 1969; Jungers, 1988). This hip morphology is thought to help dissipate the increased load that occurs when supporting body mass over two, rather than four, limbs. Biomechanical studies have revealed that the peak contact force on the human hip during walking is directed posteriorly, laterally and inferiorly (Pedersen et al. 1997) and is located at the posterior aspect (Paul, 1976; English & Kilvington, 1979). Furthermore, pressure on the acetabulum is mainly located posteriorly during different activities, such as standing up or sitting down (Yoshida et al. 2006). Lack of congruence between the femoral head and the acetabulum, combined with an anterior-facing acetabulum, results in the anterior region of the femoral head not being fully covered by the acetabulum during bipedal locomotion (Hogervorst et al. 2009; Bonneau et al. 2014). Thus, the anterior regions of the femoral head and acetabulum play a smaller role in load transmission compared with other regions of the hip joint.

Examining the potential links between internal femoral bone structure and extant ape locomotion will greatly facilitate attempts to reconstruct the locomotion of extinct hominins (e.g. Skinner et al. 2015). Here we provide this comparative context by analysing the trabecular architecture throughout the entire femoral head in extant great apes and humans that vary in their locomotor behaviours. We quantify BV/TV, DA, trabecular number (Tb.N), trabecular separation (Tb.Sp) and trabecular thickness (Tb.Th) throughout the femoral head. Based on the locomotor and biomechanical studies reviewed above, we make the following predictions regarding species variation in femoral head trabecular structure.

BV/TV distribution in the femoral head

The distribution of BV/TV throughout the femoral head will reflect joint positioning and loading during habitual locomotion. In *Pan* we expect high BV/TV to extend from the posterior and superior aspects of the femoral head to the anterior region, reflecting hip angles and loading during knuckle-walking locomotion and vertical climbing (Isler, 2005; Finestone et al. 2018). We predict that *Gorilla* will show a similar pattern of BV/TV distribution, although the region of high BV/TV is expected to extend over a smaller area of the femoral head compared with that of *Pan*, reflecting a reduced range of motion (Hammond, 2014) and different flexion/extension angles at the *Gorilla* hip during knuckle-walking and climbing (Isler, 2005; Finestone et al. 2018). We predict that *Pongo* will show the most variable BV/TV distribution pattern, reflecting loading of the femoral head at different hip joint angles, with high BV/TV spanning the whole of the superior area of the femoral head. Finally, we expect a more restricted region of high BV/TV in *Homo* that will be concentrated superiorly and posteriorly on the femoral head, reflecting the stereotypical loading pattern of bipedal locomotion.

Mean trabecular parameters in the femoral head

We hypothesise that relative interspecific differences in mean BV/TV values will be consistent with those of previous trabecular studies on the femur (e.g. Georgiou et al. 2018; Ryan et al. 2018; Tsegai et al. 2018) and other postcranial elements (e.g. Maga et al. 2006; Cotter et al. 2009; Scherf et al. 2013; Tsegai et al. 2013, 2017), such that *Pan* will have the highest BV/TV and *Homo* will have the lowest, with *Gorilla and Pongo* intermediate between these two taxa. Furthermore, mean DA of the entire femoral head will reflect the range of motion of the hip joint during habitual locomotion. *Pan* and *Gorilla* will display intermediate DA values, showing less anisotropic femoral heads than *Homo*, because they engage in both terrestrial and arboreal behaviours that employ an increased range of motion at the hip. *Pongo* will be the most isotropic, reflecting their highly mobile hip joint and diverse positioning of the proximal femur during their varied quadrumanous locomotor behaviours. *Homo* will be the most anisotropic, consistent with more stereotypical loading of the hip joint during bipedal locomotion.

In addition to BV/TV and DA, we quantify mean Tb.N, Tb.Sp and Tb.Th within the femoral head to better understand potential variation in the trabecular architecture across our sample and for comparison with previous studies (e.g. Ryan & Shaw, 2012, 2015; Ryan et al. 2018). In primates, these parameters scale negatively allometrically with body size (Barak et al. 2013a; Ryan & Shaw, 2013) meaning results may be affected by body mass. BV/TV and DA are expected to better reflect functional adaptations, as DA does not scale with body mass and BV/TV shows either no relationship (Doube et al. 2011; Barak et al. 2013a) or a

weak positively allometric relationship (Ryan & Shaw, 2013) with body mass.

Methodology

Study sample

Microcomputed tomographic scans were used to analyse trabecular morphology in the femoral head of great apes and humans. Details of the study sample are provided in Table 1. The *P. troglodytes* sample ($n = 20$) comprises two subspecies: *Pan troglodytes verus* ($n = 15$) from the Taï Forest collection curated at the Max Planck Institute for Evolutionary Anthropology in Leipzig, Germany, and *Pan troglodytes troglodytes* ($n = 5$) curated at the Smithsonian National Museum of Natural History in Washington, D.C., USA. The *Gorilla gorilla gorilla* sample ($n = 14$) is from the Powell-Cotton Museum, UK, of which 13 individuals are from Cameroon and one is from the Democratic Republic of the Congo. The *Pongo* sample ($n = 5$ and all female) is from the Zoologische Staatssammlung München, Germany: four of the individuals are *Pongo pygmaeus* and one is *Pongo pygmaeus abelii*. The *H. sapiens* sample ($n = 12$) is curated at the Georg-August-Universität Göttingen, Germany. Ten of the individuals come from a Catholic cemetery in Göttingen, which was used between 1851 and 1889, and two come from a cemetery in the village of Inden that was used between 1877 and 1924. All specimens were adult, based on complete epiphyseal fusion throughout the skeleton, and none showed obvious signs of pathology.

The *Pan*, *Pongo* and *Homo* samples were scanned at the Department of Human Evolution in the Max Planck Institute for Evolutionary Anthropology, Leipzig, Germany, using a BIR ACTIS 225/300 industrial microCT scanner. The *Gorilla* sample was scanned at the Cambridge Biotomography Centre in the Department of Zoology at the University of Cambridge, Cambridge, UK, using a Nikon XT 225 ST microCT scanner. All specimens were scanned at the highest possible resolution based on the size of the bone, ranging from 0.029 to 0.082 mm, and were reconstructed into 16-bit TIFF stacks with isometric voxel sizes. Reconstructed datasets were re-oriented to the same anatomical position and cropped in AVIZO 6.3® (Visualization Sciences Group, SAS). All specimens, except six gorillas, were re-sampled due to computational limitations of MEDTOOL 4.1(www.dr-pahr.at) and resultant resolutions are given in Table 1. Bone was segmented from air using the Ray Casting Algorithm (Scherf & Tilgner, 2009).

Trabecular architecture analysis

Patterns of trabecular bone distribution throughout the whole femoral head were analysed in MEDTOOL 4.1 (www.dr-pahr.at), following the protocol described by Gross et al. (2014). A series of morphological filters were applied to identify and remove the cortical shell, thus isolating the trabecular structure. The resulting isolated trabecular structure was used to calculate trabecular thickness using the BoneJ plug-in (version 1.4.1, Doube et al. 2010) for IMAGEJ (Schneider et al. 2012) to validate the parameters used in the morphological filters for the separation of the cortical shell (see Gross et al. 2014). The original dataset and trabecular structure were used to create a trinary mask defining the outer air, inner air and trabecular bone. A 3D rectangular background grid with a size of 3.5 mm was superimposed on the trabecular structure and a sphere with a diameter of 7.5 mm was used to measure BV/TV at each node in MEDTOOL 4.1. BV/TV was calculated as the ratio of bone to total volume in the sampling spheres. The isolated trabecular structure and a mesh size of 0.6 mm were used to create 3D tetrahedral meshes of all individuals, using CGAL 4.4 (CGAL, Computational Geometry, http://www.cgal.org) and BV/TV values were then interpolated on the tetrahedral elements of each mesh. Distribution maps of BV/TV were visualised using PARAVIEW v4.0.1 (Ahrens et al. 2005). The femoral head for each specimen was manually isolated in AVIZO 6.3® by positioning the mediolateral axis facing superoinferiorly and cropping at the head-neck junction to ensure homology across specimens. Trabecular parameters (BV/TV, DA, Tb.N, Tb.Sp, Tb.Th) for the femoral head were calculated using an in-house script in MEDTOOL 4.1. Mean BV/TV, DA, Tb.Sp and Tb.Th were quantified within the entire epiphysis, and Tb.N was calculated from the means of Tb.Sp and Tb.Th. DA was calculated as DA = 1 − (smallest eigenvalue/largest eigenvalue), as they were calculated using the mean-intercept-length method (Whitehouse, 1974; Odgaard, 1997). Tb.Sp and Tb.Th were calculated based on the Hildebrand & Rüegsegger (1997) method; Tb.N was then calculated as $Tb.N = 1/(Tb.Th + Tb.Sp)$.

Statistical analysis

Statistical analysis was performed in R v3.4.1 (R Development Core Team, 2017). The Kruskal–Wallis test was used to evaluate interspecies differences in mean trabecular parameters (BV/TV, DA, Tb.N, Tb.Sp, Tb.Th) of the femoral head, and a Wilcoxon rank sum test with Bonferroni correction was used for *post-hoc* pairwise comparisons.

Table 1 Study sample taxonomic composition, re-sampled voxel size range, sex and microCT scanning parameters.

Taxon	Locomotor mode	*n*	Sex	Voxel size (mm)	Scanning
Pan troglodytes	Arboreal/knuckle-walker	20	13 female, 6 male, 1 unknown	0.04–0.05	kV: 120–130, μA: 80–100, 0.25 or 0.5 mm brass
Gorilla gorilla gorilla	Terrestrial knuckle-walker	14	7 female, 7 male	0.05–0.08	kV: 130–170, μA: 110–160, 0.1–0.5 mm copper
Pongo sp.	Arboreal/torso-orthograde suspension	5	5 female	0.04–0.045	kV: 140, μA: 140, 0.5 mm brass
Homo sapiens	Bipedal	12	3 female, 8 male, 1 unknown	0.06–0.07	kV: 130–140, μA: 100–140, 0.5 mm brass

All specimens were re-sampled except six of the gorillas that were scanned at lower resolutions.

Results

BV/TV distribution in the femoral head

In *Pan*, BV/TV distribution maps of the femoral head reveal concentrations of high BV/TV in the superior aspect of the femoral head (Fig. 2). In most *Pan* individuals (n = 12) there are two distinct concentrations, one located more posteriorly and one more anteriorly, whereas in some individuals one concentration spans the whole of the superior region of the articulation. Whereas the posterior concentration is always present in *Pan*, the location, extent and isolation of the anterior concentration vary between individuals.

The pattern of BV/TV distribution in *Gorilla* is similar to that found in *Pan* (Fig. 3). Two concentrations of high BV/TV are seen in the superior aspect, one located anteriorly and one posteriorly. Unlike in *Pan,* however, these concentrations are distinct from each other in all but three *Gorilla* individuals, in which a region of high BV/TV spans the superior region of the femoral head. There is no apparent difference in the size of the two regions of high BV/TV.

Pongo shows a slightly different BV/TV pattern compared with *Pan* and *Gorilla* (Fig. 4). The *P. pygmaeus* individuals show the two concentrations of high BV/TV, one in the anterior and one in the posterior, similar to what is found in the African apes; however, intermediate values persist over the superior portion of the femoral head. The extent of this concentration differs between *P. pygmaeus* individuals: in two individuals it is restricted more in the superior aspect of the head, whereas in the other two it is enlarged and covers the majority of the femoral head, from the anterior to the posterior. When the two concentrations are more well-defined, the posterior concentration is generally more mediolaterally expanded than the anterior concentration. The *P. abelii* individual shows lower BV/TV than the other specimens and does not show two distinct concentrations.

Homo shows a different pattern to the great apes (Fig. 5). All individuals show one region of high BV/TV located in the posterior and superior aspect of the femoral head. Intermediate values of BV/TV expand across the whole of the superior aspect of the head of *Homo*, but not with the apparent second concentration of high BV/TV in the anterior region that is found in great apes. *Homo* individuals also display intermediate BV/TV on the inferior aspect of the head. This expansion of intermediate BV/TV values along the inferior is not seen in the other apes.

Quantitative analysis of trabecular parameters in the femoral head

Quantitative analysis of the mean trabecular parameters over the femoral head revealed several differences across taxa. Results for each parameter in the different taxa are presented in Table 2 and statistical results of species pairwise comparisons, after Bonferroni corrections, are presented in Table 3. *Pan* shows significantly higher BV/TV in the femoral head than *Pongo* ($P = 0.05$) and *Homo* ($P < 0.001$), and although its mean BV/TV value was higher than that of *Gorilla*, this difference was not statistically significant (Tables 2 and 3). *Homo* has the lowest mean BV/TV of all the great apes but is only significantly different from *Pan*. *Homo* has significantly higher DA in the femoral head than all other apes (*Pan* $P < 0.001$; *Gorilla* $P < 0.05$; *Pongo* $P < 0.01$). *Pan, Pongo* and, less so, *Gorilla* are more isotropic and not significantly different from each other. With regard to the architectural parameters, *Pan* shows the most distinct trabecular structure with significantly higher Tb.N than all other apes (*Gorilla* $P < 0.001$; *Homo* $P < 0.001$; *Pongo* $P < 0.01$) and significantly lower Tb.Sp (all $P < 0.001$) and lower Tb.Th than *Gorilla* ($P < 0.001$) and *Homo* ($P < 0.05$).

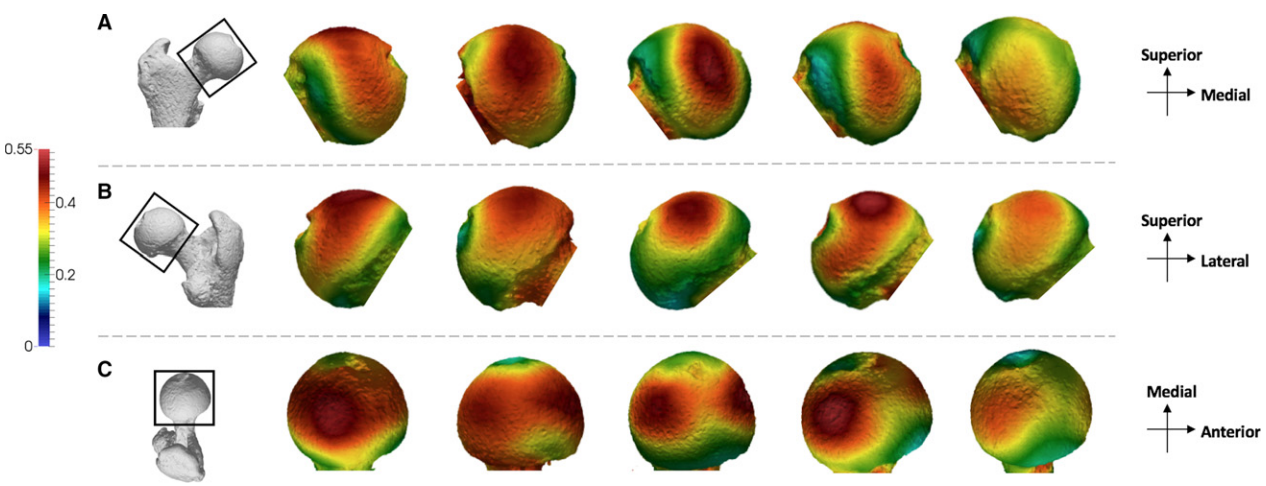

Fig. 2 *Pan* BV/TV distribution in the femoral head. Five *Pan* specimens showing variation in the BV/TV distribution across the sample in (A) anterior, (B) posterior and (C) superior views. BV/TV is scaled to 0–0.55. All specimens are from the right side. Specimens from left to right (F, female; M, male): MPITC 14996 (F), USNM 220063 (F), USNM 176228 (M), MPITC 11781 (M), MPITC 11786 (F).

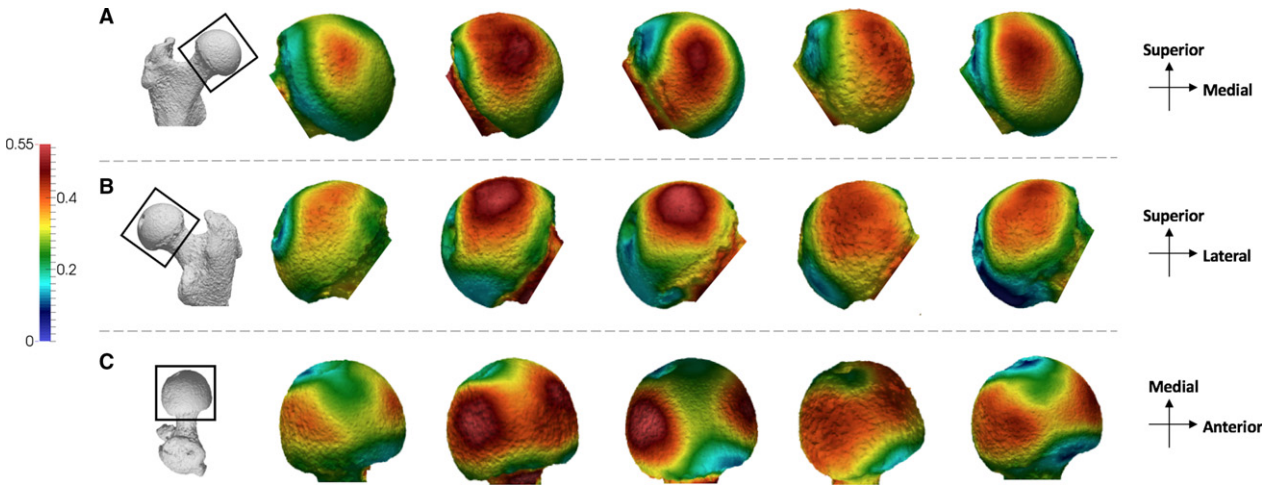

Fig. 3 *Gorilla* BV/TV distribution in the femoral head. Five *Gorilla* specimens showing variation in the BV/TV distribution across the sample in (A) anterior, (B) posterior and (C) superior views. BV/TV is scaled to 0–0.55. All specimens are from the right side. Specimens from left to right (F, female; M, male): M96 (F), M264 (M), M372 (M), M856 (F), FC123 (M).

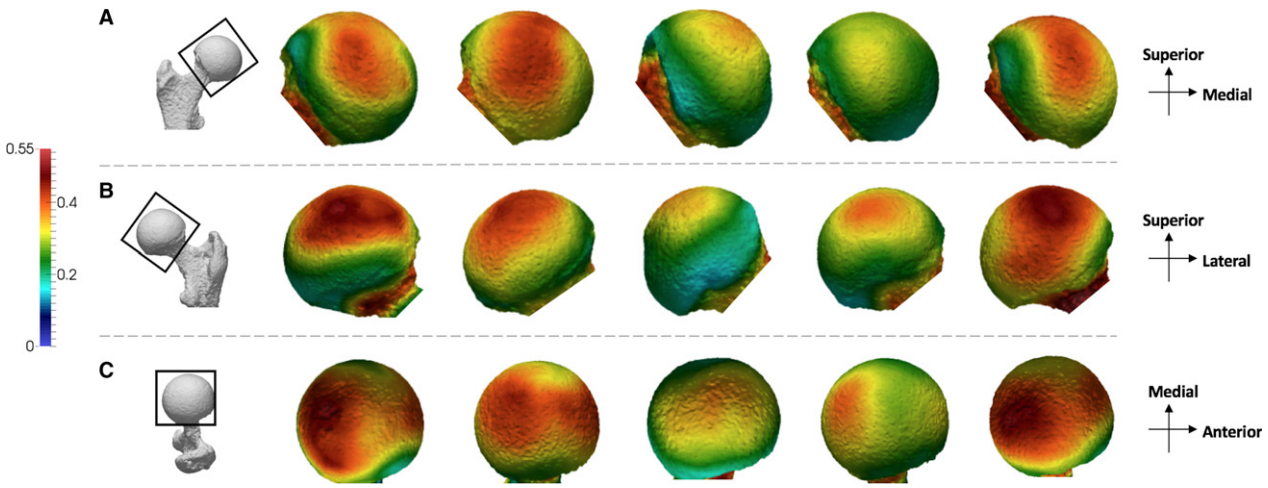

Fig. 4 *Pongo* BVTV distribution in the femoral head. Five *Pongo* specimens showing variation in the BV/TV distribution across the sample in (A) anterior, (B) posterior and (C) superior views. BV/TV is scaled to 0–0.55. All specimens are from the right side. Specimens from left to right (All female): ZSM 1909 0801, 1907 0660, 1973 0270, 1907 0483, 1907 0633b.

Differences in mean BV/TV and DA across taxa were further evaluated using a bivariate plot (Fig. 6) and a line histogram of the distribution of values in each taxon (Fig. 7). The data depicted in these figures are mean values for each individual across the entire femoral head. In the bivariate plot, *Pan* shows a combination of high BV/TV and low DA, in contrast to humans that show the opposite pattern. *Gorilla* overlaps with both of these taxa but shows higher BV/TV than humans. *Pongo* individuals overlap with the African apes, with lower DA values than humans, but with BV/TV values that overlap with all other taxa.

These differences are reflected in the distribution of BV/TV and DA values in the taxa (Fig. 7). *Pan* shows the highest mean BV/TV, with individuals close to the mean (0.39), whereas *Gorilla* shows a lower mean value but most individuals are between 0.3 and 0.4. *Pongo* shows a similar mean to *Gorilla*, but the distribution of values more closely resembles that of *Pan*. *Homo* shows the lowest BV/TV values distributed over a wider area. The DA plot shows that *Pan, Gorilla* and *Pongo* present similarly low mean DA values, but *Pongo* differs in distribution with more individuals around the mean. *Homo* shows a different distribution with the highest mean DA but a wider distribution of values in the sample.

Discussion

Our study investigated the variation in trabecular patterns of the femoral head in great apes and humans. Qualitative and quantitative results supported our hypotheses that

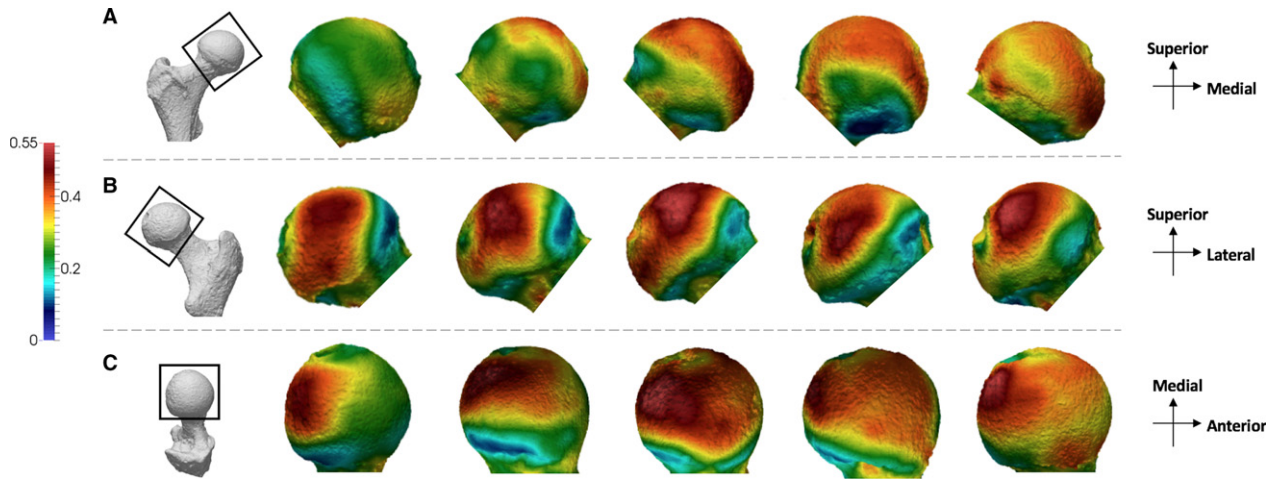

Fig. 5 *Homo* BV/TV distribution in the femoral head. Five *Homo* specimens showing variation in the BV/TV distribution across the sample in (A) anterior, (B) posterior and (C) superior views. BV/TV is scaled to 0–0.55. All specimens are from the right side. Specimens from left to right (F, female; M, male): CAMPUS 36 (F), CAMPUS 93 (M), CAMPUS 74 (F), CAMPUS 417 (sex unknown), CAMPUS 81 (M).

Table 2 Trabecular architecture results.

Taxon	*Pan*	CV	*Gorilla*	CV	*Pongo*	CV	*Homo*	CV
BV/TV	0.39 (0.03)	8.6	0.35 (0.05)	14.8	0.33 (0.04)	13.4	0.30 (0.05)	16.0
DA	0.15 (0.03)	21.6	0.18 (0.04)	21.8	0.15 (0.02)	14.7	0.23 (0.04)	17.9
Tb.N (1 mm^{-1})	1.19 (0.11)	9.4	0.83 (0.09)	10.7	0.92 (0.04)	4.4	0.87 (0.1)	11.4
Tb.Sp (mm)	0.56 (0.06)	10.0	0.81 (0.08)	9.8	0.78 (0.07)	8.4	0.84 (0.14)	16.6
Tb.Th (mm)	0.29 (0.03)	11.8	0.40 (0.08)	19.1	0.31 (0.03)	10.9	0.32 (0.03)	9.9

Mean, standard deviation (in parentheses) and coefficient of variation (CV) for five trabecular parameters quantified throughout the femoral head.

Table 3 Results of pairwise comparisons between taxa.

	Pan – *Gorilla*	*Pan* – *Pongo*	*Pan* – *Homo*	*Gorilla* – *Pongo*	*Gorilla* – *Homo*	*Pongo* – *Homo*
BV/TV	0.14	< 0.05	< 0.001	1	0.14	1
DA	0.24	1	< 0.001	1	< 0.05	< 0.01
Tb.N	< 0.001	< 0.01	< 0.001	0.33	1	1
Tb.Sp	< 0.001	< 0.001	< 0.001	1	1	1
Tb.Th	< 0.001	1	< 0.05	0.09	0.05	1

Bonferroni-corrected *P*-values of each pairwise comparison for all trabecular parameters.

trabecular bone would reflect differences in locomotor patterns, but not necessarily in the way we predicted. *Pan* and *Gorilla* displayed trabecular structures consistent with their terrestrial as well as arboreal quadrupedal locomotion, whereas *Homo* showed a distinct trabecular pattern indicative of stereotypical loading during bipedal locomotion. However, the African apes showed a BV/TV distribution pattern that was different to what was expected, and their trabecular structure did not differ significantly from *Pongo*.

Distribution of BV/TV within the femoral head

We predicted that African apes would display a region of high BV/TV extending from the posterosuperior to the anterior region of the femoral head, reflecting the flexed hip postures and loading incurred during knuckle-walking and vertical climbing. However, instead of a continuous band of high BV/TV across the femoral head, *Pan* displayed two main regions of high BV/TV, indicating two regions of high loading: one in the posterosuperior aspect of the femoral

head and one located more anteriorly. The majority of Taï chimpanzee (75% of the *Pan* sample) locomotion is terrestrial quadrupedalism (Doran, 1993a,b). Ground reaction forces remain high throughout the stance phase during terrestrial knuckle-walking (Barak et al. 2013b) and the hip remains flexed (Finestone et al. 2018), both of which are consistent with high loading of the posterosuperior region of the femoral head and the high BV/TV concentration that was found in this region. Although Taï chimpanzees engage less frequently in vertical climbing (Doran, 1993a), it is possible that this results in similarly high loading of the femoral head, as it involves high propulsive forces from the hindlimbs (Hanna et al. 2017). During climbing, the hip can be flexed to a maximum of 25°–55° (Isler, 2005; Nakano et al. 2006), which would result in the anterior aspect of the head contacting the lunate surface of the acetabulum. This is consistent with the second region of high BV/TV found in the anterior portion of the femoral head in *Pan*. The anterior concentration was more variable between individuals, but this could not be explained by subspecies differences within the sample. Thus, the more variable anterior BV/TV pattern may reflect interindividual variability in vertical climbing frequency (Doran, 1993b) or hip range of motion during climbing (Isler, 2005; Nakano et al. 2006).

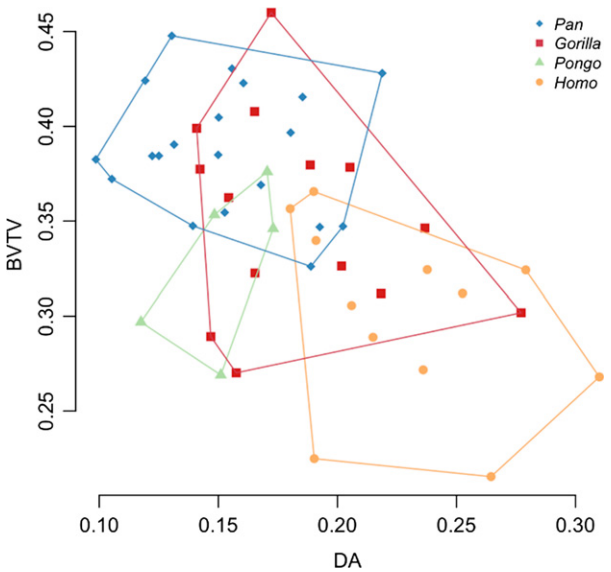

Fig. 6 Bivariate plot of mean bone volume fraction (BV/TV) and mean degree of anisotropy (DA) for each individual and species in the sample.

Gorilla displayed a similar pattern to *Pan*, with two regions of high BV/TV within the femoral head. The two regions, one in the posterior and one in the anterior aspect of the head, are, as in *Pan*, consistent with hip posture and loading during terrestrial quadrupedalism and vertical climbing, as these modes of locomotion comprise the majority of *Gorilla* locomotion (Remis, 1995; Doran, 1997; Crompton et al. 2010). However, unlike *Pan*, these regions were better defined and more discrete in most *Gorilla* individuals (11 of 14 individuals). This more discrete pattern is perhaps due to their greater body mass. Greater mass is related to restricted range of motion in joints (Hammond, 2014), which could result in less variability in joint positioning during locomotion and may explain the more well-defined concentrations in *Gorilla*. The two concentrations appeared closer to each other in *Gorilla* than in *Pan*, which is also consistent with the reduced range of motion at the hip joint of *Gorilla* (Isler, 2005; Hammond, 2014). Significant sex- and body size-related differences in joint mobility are prominent in *Gorilla*, with females showing a larger range of motion than males, and flexion-extension ranges varying between the sexes by up to or even more than 30° (Isler, 2005; Hammond, 2014). These differences were not detected in the BV/TV distribution maps and *Gorilla* does not seem to be more variable than *Pan*. However, this could not be tested statistically in the current study.

We predicted that the BV/TV distribution pattern of the *Pongo* femoral head would differ from that of African apes and humans because of their more varied quadrumanous

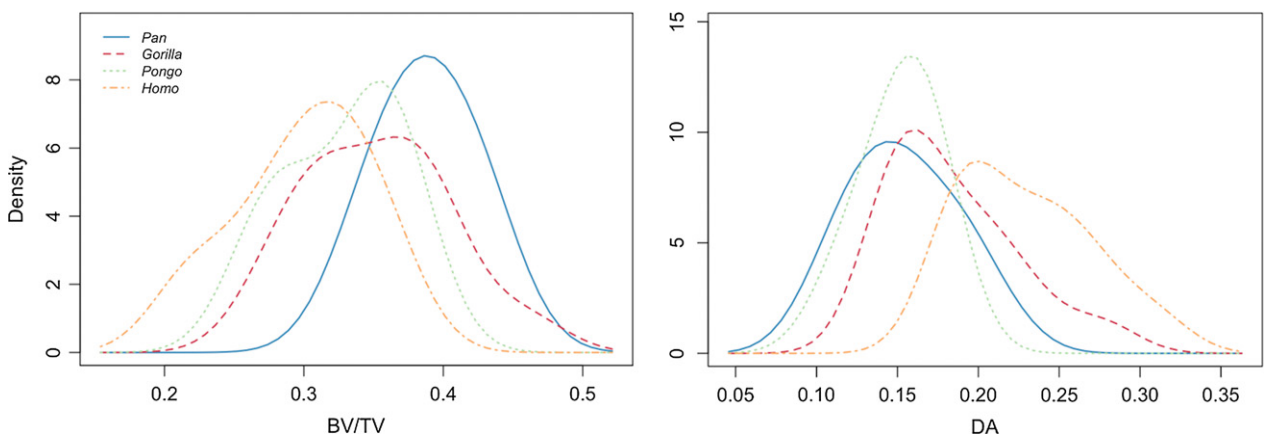

Fig. 7 A histogram of mean BV/TV and DA value distributions in the studied taxa.

locomotor behaviours (Thorpe & Crompton, 2005, 2006), more mobile hip joints (Crelin, 1988; Ward, 1991), and increased range of motion at the hip during vertical climbing compared with African apes (Isler, 2005). Four of the five *Pongo* individuals in our sample showed the same two regions of high BV/TV found in African apes; however, these were not as distinct and, instead, there was a continuous concentration of BV/TV spanning the superior aspect of the femoral head. This is perhaps unsurprising, as *Pongo* uses a variety of hip postures while navigating their arboreal environment (Thorpe & Crompton, 2005, 2006; Payne et al. 2006; Thorpe et al. 2009), which potentially results in higher loading across the whole superior surface of the femoral head. *Pongo* also less frequently climbs vertically than African apes do (Thorpe & Crompton, 2006), which may be reflected by the less defined anterior concentration of high BV/TV in *Pongo* compared with *Pan* and, especially, with *Gorilla*. Although our sample of *Pongo* is small ($n = 5$) and all individuals were female, there was greater variation in the BV/TV distributions along the anterior and posterior aspects of the femoral head than was found in African apes. The one *P. abelii* specimen in our sample differed from the *P. pygmaeus* individuals in having only one superior concentration of high BV/TV. Although locomotor differences have been documented between *P. pygmaeus* and *P. abelii* (Sugardjito & van Hooff, 1986; Cant, 1987), a larger sample of both species is needed to determine whether this variation in the trabecular pattern is characteristic of each species.

Homo showed a distinct trabecular pattern that is consistent with our predictions and similar to previous results showing the density distribution of trabeculae adjacent to cortical bone (Treece & Gee, 2014). All *Homo* individuals displayed one main region of high BV/TV, located posteriorly and superiorly on the femoral head. This concentration was positioned more medially than the posterior concentration seen in great apes and closer to the fovea capitis, which is consistent with loading of the femur at a valgus angle. Intermediate BV/TV values continued along the superior aspect of the femoral head in *Homo*. This is consistent with loading that occurs throughout the gait cycle over the articulating surface but suggests that peak loading is occurring at the posterosuperior region, which is in contact with the acetabulum during walking (Bonneau et al. 2012, 2014). Of course, humans also engage in other activities that involve more flexed hip joint postures, such as running, jumping or climbing stairs, all of which impose high loads on the lower limb (Van der Bogert et al. 1999; Giarmatzis et al. 2015) and could result in some trabecular reorganisation, explaining the extended area of intermediate BV/TV values we found across the femoral head. Unfortunately, it is not yet known exactly how the peak load is distributed over the femoral head during these activities. However, all individuals lack the anterior concentration found in apes, further supporting the interpretation that high BV/TV in the anterior region could be linked to arboreal behaviours or, more specifically, vertical climbing.

Quantitative analysis of trabecular structure

Quantitative analysis of the femoral head trabecular structure only partially supported our hypotheses. As expected, *Homo* displayed the lowest mean BV/TV in our sample but was only significantly different from that of *Pan*. Our results confirm previous studies showing that modern humans, particularly those that are less active, have relatively lower BV/TV across the skeleton compared with highly mobile modern humans and other primates (Chirchir et al. 2015, 2017; Ryan & Shaw, 2015; Saers et al. 2016). Furthermore, *Homo* showed significantly higher DA than great apes, which is consistent with the more stereotypical loading of the hip joint during bipedal locomotion and in accordance with previous results from the proximal (Ryan & Shaw, 2015; Ryan et al. 2018) as well as the distal femur (Georgiou et al. 2018). *Homo* has narrower acetabulae than other great apes, with expanded cranial lunate surfaces, as well as shortened dorsal surfaces, which result in a distinctively shaped dorso-cranially expanded lunate surface that may restrict movement in the parasagittal plane (San Millán et al. 2015). Furthermore, in *Homo* the iliofemoral ligament limits extension and external rotation (Myers et al. 2011), the ischiofemoral ligament limits internal rotation, and the pubofemoral ligament limits abduction (Wagner et al. 2012), all of which result in a more restrictive and stereotypical motion and loading of the femoral head that is reflected in the trabecular structure.

As predicted, mean BV/TV was highest in *Pan*, which is consistent with previous studies showing relatively high BV/TV in the African ape femur (Ryan & Shaw, 2015; Georgiou et al. 2018; Ryan et al. 2018; Tsegai et al. 2018) and other postcranial elements (e.g. Cotter et al. 2009; Scherf et al. 2013; Tsegai et al. 2017). BV/TV in *Pan* did not differ significantly from *Gorilla*, reflecting their generally similar locomotor repertoire. Overall, the quantitative analysis highlighted *Pan* as being distinct from the other taxa. *Pan* not only showed the highest BV/TV values, but also differed significantly from all taxa in Tb.N and Tb.Sp, showing consistently higher Tb.N and lower Tb.Sp, again resembling previous findings (Ryan & Shaw, 2015). Furthermore, *Pan* showed significantly lower Tb.Th than *Gorilla* and *Homo* did. Additionally, mean DA was lowest in *Pan* as well as *Pongo*, but only differed significantly from *Homo*. Fewer data are available on the femoral ligaments of non-human apes; however, *Pan* and *Pongo* seem to have less restrictive ligaments than *Homo* do (Sonntag, 1923, 1924).

The trabecular structure of *Gorilla* and *Pongo* was not as distinct. *Gorilla* BV/TV means did not differ significantly from any other taxon, and they only differed significantly in Tb.N, Tb.Sp and Tb.Th from *Pan*, as well as in DA from *Homo*. *Gorilla* has less variable positioning of their lower

limbs during locomotion, compared with other non-human apes, as was shown in vertical climbing (Isler, 2005); however, this is not displayed as clearly in their DA values as was initially predicted. The lack of significant differences in BV/TV and DA with *Pan* can perhaps be explained by the similar shape of their hip joints (San Millán et al. 2015) and overall similarities in locomotion (Doran, 1997). None of great apes differed significantly in DA, despite clear differences in locomotor behaviours and hip morphology. *Pongo* has a cranio-ventrally expanded lunate surface and a smaller acetabular fossa compared with other apes. They also show the largest articular surfaces and relatively shallow acetabulae (Schultz, 1969), which may be responsible for the increased mobility of the femoral head. Furthermore, *Pongo* has a greater capacity for abduction and external rotation than non-suspensory taxa (Hammond, 2014). Thus, *Pongo* was expected to display significantly lower DA values than all other taxa, which was not the case, but this result may also reflect our small sample size for this taxon.

Our results showed that *Pan* has relatively numerous, thinner and compactly organised trabeculae, whereas *Gorilla* and *Homo* have relatively few, thicker and more separated trabeculae. *Pongo* has relatively few, thinner and more separated trabeculae. These results are largely in accordance with previous analyses of femoral head trabeculae (Ryan & Shaw, 2012, 2015) which showed that humans have relatively less numerous, thin and highly anisotropic trabeculae compared with other anthropoids, *Pan* has relatively high numbers of thick, isotropic trabeculae and *Pongo* have relatively few, isotropic trabeculae. *Gorilla* showed the thickest trabeculae (Table 2), in support of previous studies suggesting that larger taxa have absolutely thicker trabeculae (Barak et al. 2013a; Ryan & Shaw, 2013; Tsegai et al. 2013). However, the difference was not found to be significant, possibly due to the small sample sizes in our study. Allometric relationships were not tested in our study because our sample sizes were not large enough to test this intraspecifically; however, previous research has shown that these trabecular parameters can vary predictably with body size interspecifically (Cotter et al. 2009; Doube et al. 2011; Barak et al. 2013a; Ryan & Shaw, 2013). Across a large sample of mammals, Tb.Th and Tb.Sp were shown to increase with size (Doube et al. 2011). In primates, Tb.N, Tb.Th and Tb.Sp present negatively allometric relationships with body mass (Barak et al. 2013a; Ryan & Shaw, 2013), resulting in more, thinner and less separated trabeculae in larger taxa. These studies suggest that absolute trabecular parameters, and specifically Tb.N, Tb.Sp and Tb.Th, do not necessarily directly reflect locomotor modes as they could reflect body-size related or systemic differences between taxa. Nevertheless, as our sample includes apes that are relatively similar in body size compared with the more diverse samples of previous studies (Doube et al. 2011; Barak et al. 2013a; Ryan & Shaw, 2013), we would expect that allometry does not have a significant effect on the variation observed here.

The absence of a clear functional signal in the mean trabecular parameters may be due to methodological limitations of the whole-epiphysis approach. The mean value of any given trabecular parameter can obscure or homogenise any potential distinct variation in specific regions of the femoral head, as demonstrated by the BV/TV distribution maps and previous studies (Sylvester & Terhune, 2017). This is where the traditional VOI approach, in which the trabecular architecture of specific regions of an epiphysis can be quantified and compared, is potentially more functionally informative (e.g. Ryan & Shaw, 2012, 2015; Ryan et al. 2018). Additionally, the lack of a strong functional signal in these parameters could be due to non-mechanical factors affecting trabecular structure. Trabecular bone also functions as a reserve of minerals and is important in maintaining homeostasis, hence its structure will, to some extent, be affected by this (Rodan, 1998; Clarke, 2008). Genes control for the rate of remodelling and bone mineral density, as well as the response to mechanical strain in different skeletal sites (Smith et al. 1973; Dequeker et al. 1987; Kelly et al. 1991; Garnero et al. 1996; Hauser et al. 1997; Harris et al. 1998; Judex et al. 2002, 2004). These factors, along with the fact that trabecular bone remodels in response to a range of magnitudes and frequencies of load (Whalen et al. 1988; Rubin et al. 1990, 2001; Judex et al. 2003; Scherf et al. 2013), complicate interpretations. Age, hormones, sex and other factors (e.g. Simkin et al. 1987; Pearson & Lieberman, 2004; Suuriniemi et al. 2004; Kivell, 2016; Wallace et al. 2017; Tsegai et al. 2018) influence trabecular bone modelling and thus should not be ignored. Nonetheless, future research will aim to use techniques that will allow statistical comparisons of the trabecular distribution patterns in the femoral head of apes, rather than mean parameters, for more accurate interpretation of locomotor patterns in extinct hominins.

Conclusion

This study showed that the trabecular architecture of the femoral head in great apes and humans reflects habitual hip postures during locomotion. *Pan* and *Gorilla* showed similar BV/TV distribution patterns, with generally two distinct high BV/TV regions that are consistent with hip postures during knuckle-walking and vertical climbing. *Pongo* showed a BV/TV distribution pattern that is characteristic of their highly mobile hips and complex locomotion; however, they do not differ as significantly as predicted from African apes. Finally, *Homo* showed a distinct pattern of BV/TV distribution, with one posterosuperior region of high BV/TV, the lowest overall BV/TV values and the highest DA values, which is consistent with stereotypical loading during locomotion. Despite mean trabecular parameters not demonstrating locomotor differences as clearly as predicted, they

largely match results from previous VOI studies (Ryan & Shaw, 2015; Ryan et al. 2018). Our research reveals that there are distinct patterns of BV/TV distribution that generally distinguish the locomotor groups and provide a valuable comparative sample for future research on the evolution of gait in hominins.

Acknowledgements

We thank the following researchers for access to specimens: Anneke Van Heteren (Zoologische Staatssammlung München), Inbal Livne (Powell-Cottom Museum), Christophe Boesch and Jean-Jacques Hublin (Max Planck Institute for Evolutionary Anthropology), and Brigit Grosskopf (Georg-August University of Goettingen). We also thank David Plotzki (Max Planck Institute for Evolutionary Anthropology) and Keturah Smithson (University of Cambridge) for the CT scanning of specimens. We thank Zewdi Tsegai for facilitating access to CT data and Kim Deckers for discussions that improved this manuscript. We are grateful to two anonymous reviewers for their valuable feedback that improved this manuscript. This research is supported by a 50th Anniversary Research Scholarship, University of Kent (L.G.), European Research Council Starting Grant 336301 (M.M.S., T.L.K.), and the Max Planck Society (M.M.S., T.L.K).

Authors' contributions

L. Georgiou, T. L. Kivell and M. M. Skinner contributed to the design of the study and acquisition of data. L. T. Buck facilitated and collected data. D. H. Pahr contributed to the analysis tools. L. Georgiou processed, analysed and interpreted the data, and drafted the manuscript. L. Georgiou, T. L. Kivell, D. H. Pahr, L. T. Buck and M.M. Skinner revised and approved the final manuscript submitted for review.

References

Abbass SJ, Abdulrahman G (2014) Kinematic analysis of human gait cycle. *Nahrain Univ Coll Eng J* **16**, 208–222.

Ahrens J, Geveci B, Law C (2005) ParaView: an end-user tool for large data visualization. In: *Visualization Handbook*. (eds Hansen CD, Johnson CR), pp. 717–731. Burlington: Butterworth-Heinemann.

Aiello L, Dean C (2002) *An Introduction to Human Evolutionary Anatomy*. San Diego: Academic Press.

Alexander CJ (1994) Utilisation of joint movement range in arboreal primates compared with human subjects: an evolutionary frame for primary osteoarthritis. *Ann Rheum Dis* **53**, 720–725.

Barak MM, Lieberman DE, Hublin J (2011) A Wolff in sheep's clothing: trabecular bone adaptation in response to changes in joint loading orientation. *Bone* **49**, 1141–1151.

Barak MM, Lieberman DE, Hublin J (2013a) Of mice, rats and men: trabecular bone architecture in mammals scales to body mass with negative allometry. *J Struct Biol* **183**, 123–131.

Barak MM, Lieberman DE, Raichlen D, et al. (2013b) Trabecular evidence for a human-like gait in *Australopithecus africanus*. *PLoS One* **8**, e77687.

Biewener AA, Fazzalari NL, Konieczynski DD, et al. (1996) Adaptive changes in trabecular architecture in relation to functional strain patterns and disuse. *Bone* **19**, 1–8.

Bonneau N, Gagey O, Tardieu C (2012) Biomechanics of the human hip joint. *Comput Methods Biomech Biomed Engin* **15**, 197–199.

Bonneau N, Baylac M, Gagey O, et al. (2014) Functional integrative analysis of the human hip joint: the three-dimensional orientation of the acetabulum and its relation with the orientation of the femoral neck. *J Hum Evol* **69**, 55–69.

Burr DB, Piotrowski G, Martin RB, et al. (1982) Femoral mechanics in the lesser bushbaby (*Galago senegalensis*): structural adaptations to leaping in primates. *Anat Rec* **202**, 419–429.

Cant JG (1987) Positional behavior of female Bornean orangutans (*Pongo pygmaeus*). *Am J Primatol* **12**, 71–90.

Carey TS, Crompton RH (2005) The metabolic costs of 'bent-hip bent-knee' walking in humans. *J Hum Evol* **48**, 25–44.

Carlson KJ, Lublinsky S, Judex S (2008) Do different locomotor modes during growth modulate trabecular architecture in the murine hind limb? *Integr Comp Biol* **48**, 385–393.

Chirchir H, Kivell TL, Ruff CB, et al. (2015) Recent origin of low trabecular bone density in modern humans. *Proc Natl Acad Sci U S A* **112**, 366–371.

Chirchir H, Ruff CB, Junno JA, et al. (2017) Low trabecular bone density in recent sedentary modern humans. *Am J Phys Anthropol* **162**, e23138.

Clarke B (2008) Normal bone anatomy and physiology. *Clin J Am Soc Nephrol* **3**, 131–139.

Cotter MM, Simpson SW, Latimer BM, et al. (2009) Trabecular microarchitecture of hominoid thoracic vertebrae. *Anat Rec* **292**, 1098–1106.

Crelin ES (1988) Ligament of the head of the femur in the orangutan and Indian elephant. *Yale J Biol Med* **61**, 383–388.

Crompton RH, Weijie LYW, Günther M, et al. (1998) The mechanical effectiveness of erect and 'bent-hip, bent-knee' bipedal walking in *Australopithecus afarensis*. *J Hum Evol* **35**, 55–74.

Crompton RH, Sellers WI, Thorpe SKS (2010) Arboreality terrestriality and bipedalism. *Philos Trans R Soc Lond B Biol Sci* **365**, 3301–3314.

Demes B, Larson SG, Stern JT Jr, et al. (1994) The kinetics of primate quadrupedalism: 'hindlimb drive' reconsidered. *J Hum Evol* **26**, 353–374.

Dequeker J, Nijs J, Verstraeten A, et al. (1987) Genetic determinants of bone mineral content at the spine and radius: a twin study. *Bone* **8**, 207–209.

DeSilva JM, Holt KG, Churchill SE, et al. (2013) The lower limb and mechanics of walking in *Australopithecus sediba*. *Science* **340**, 1232999.

Doran DM (1992) The ontogeny of chimpanzee and pygmy chimpanzee locomotor behavior: a case study of paedomorphism and its behavioral correlates. *Journal of Human Evolution* **23**, 139–157.

Doran DM (1993a) Comparative locomotor behavior of chimpanzees and bonobos: the influence of morphology on locomotion. *Am J Phys Anthropol* **91**, 83–98.

Doran DM (1993b) Sex differences in adult chimpanzee positional behavior: the influence of body size on locomotion and posture. *Am J Phys Anthropol* **91**, 99–115.

Doran DM (1997) Ontogeny of locomotion in mountain gorillas and chimpanzees. *J Hum Evol* **32**, 323–344.

Doube M, Kłosowski MM, Arganda-Carreras I, et al. (2010) BoneJ: free and extensible bone image analysis in ImageJ. *Bone* **47**, 1076–1079.

Doube M, Kłosowski MM, Wiktorowicz-Conroy A, et al. (2011) Trabecular bone scales allometrically in mammals and birds. *Proc Biol Sci* **278**, 3067–3073.

English TA, Kilvington M (1979) *In vivo* records of hip loads using a femoral implant with telemetric output (a preliminary report). *J Biomed Eng* **1**, 111–115.

Fajardo RJ, Müller R (2001) Three-dimensional analysis of nonhuman primate trabecular architecture using micro-computed tomography. *Am J Phys Anthropol* **115**, 327–336.

Fajardo RJ, Müller R, Ketcham RA, et al. (2007) Nonhuman anthropoid primate femoral neck trabecular architecture and its relationship to locomotor mode. *Anat Rec (Hoboken)* **290**, 422–436.

Fajardo RJ, DeSilva JM, Manoharan RK, et al. (2013) Lumbar vertebral body bone microstructural scaling in small to medium-sized strepsirhines. *Anat Rec* **296**, 210–226.

Finestone EM, Brown MH, Ross SR, et al. (2018) Great ape walking kinematics: implications for hominoid evolution. *Am J Phys Anthropol* **166**, 43–55.

Garnero P, Arden NK, Griffiths G, et al. (1996) Genetic influence on bone turnover in postmenopausal twins. *J Clin Endocrinol Metab* **81**, 140–146.

Georgiou L, Kivell TL, Pahr DH, et al. (2018) Trabecular bone patterning in the hominoid distal femur. *PeerJ* **6**, e5156.

Giarmatzis G, Ilse J, Mariska W, et al. (2015) Loading of hip measured by hip contact forces at different speeds of walking and running. *J Bone Miner Res* **30**, 1431–1440.

Gross T, Kivell TL, Skinner MM (2014) A CT-image-based framework for the holistic analysis of cortical and trabecular bone morphology. *Palaeontol Electronica* **17**, 1–13.

Gunness-Hey M, Hock JM (1984) Increased trabecular bone mass in rats treated with human synthetic parathyroid hormone. *Metab Bone Dis Relat Res* **5**, 177–181.

Hammond AS (2014) *In vivo* baseline measurements of hip joint range of motion in suspensory and nonsuspensory anthropoids. *Am J Phys Anthropol* **153**, 417–434.

Hanna JB, Granatosky MC, Rana P, et al. (2017) The evolution of vertical climbing in primates: evidence from reaction forces. *J Exp Biol* **220**, 3039–3052.

Harmon EH (2007) The shape of the hominoid proximal femur: a geometric morphometric analysis. *J Anat* **210**, 170–185.

Harmon EH (2009a) The shape of the early hominin proximal femur. *Am J Phys Anthropol* **139**, 154–171.

Harmon EH (2009b) Size and shape variation in the proximal femur of *Australopithecus africanus*. *J Hum Evol* **56**, 551–559.

Harris M, Nguyen TV, Howard GM, et al. (1998) Genetic and environmental correlations between bone formation and bone mineral density: a twin study. *Bone* **22**, 141–145.

Hauser DL, Fox JC, Sukin D, et al. (1997) Anatomic variation of structural properties of periacetabular bone as a function of age: a quantitative computed tomography study. *J Arthroplast* **12**, 804–811.

Havill LM, Allen MR, Bredbenner TL, et al. (2010) Heritability of lumbar trabecular bone mechanical properties in baboons. *Bone* **46**, 835–840.

Hildebrand T, Rüegsegger P (1997) A new method for the model-independent assessment of thickness in three-dimensional images. *J Microsc* **185**, 67–75.

Hogervorst T, Bouma HW, de Vos J (2009) Evolution of the hip and pelvis. *Acta Orthop* **80**, 1–39.

Huiskes R, Ruimerman R, van Lenthe GH, et al. (2000) Effects of mechanical forces on maintenance and adaptation of form in trabecular bone. *Nature* **405**, 704–706.

Hunt KD (1991) Positional behavior in the Hominoidea. *Int J Primatol* **12**, 95–118.

Isler K (2005) 3D-kinematics of vertical climbing in hominoids. *Am J Phys Anthropol* **126**, 66–81.

Isler K, Thorpe SKS (2003) Gait parameters in vertical climbing of captive rehabilitant and wild Sumatran orang-utans (*Pongo pygmaeus abelii*). *J Exp Biol* **206**, 4081–4096.

Jenkins FA (1972) Chimpanzee bipedalism: cineradiographic analysis and implications for the evolution of gait. *Science* **178**, 877–879.

Judex S, Donahue L, Rubin C (2002) Genetic predisposition to low bone mass is paralleled by an enhanced sensitivity to signals anabolic to the skeleton. *FASEB J* **16**, 1280–1282.

Judex S, Boyd S, Qin Y, et al. (2003) Adaptations of trabecular bone to low magnitude vibrations result in more uniform stress and strain under load. *Ann Biomed Eng* **31**, 12–20.

Judex S, Garman R, Squire M, et al. (2004) Genetically based influences on the site-specific regulation of trabecular and cortical bone morphology. *J Bone Miner Res* **19**, 600–606.

Jungers WL (1988) Relative joint size and hominoid locomotor adaptations with implications for the evolution of hominid bipedalism. *J Hum Evol* **17**, 247–265.

Keaveny TM, Morgan EF, Niebur GL, et al. (2001) Biomechanics of trabecular bone. *Annu Rev Biomed Eng* **3**, 307–333.

Kelly PJ, Hopper JL, Macaskill GT, et al. (1991) Genetic factors in bone turnover. *J Clin Endocrinol Metab* **72**, 803–813.

Kivell TL (2016) A review of trabecular bone functional adaptation: what have we learned from trabecular analyses in extant hominoids and what can we apply to fossils? *J Anat* **228**, 569–594.

Kivell TL, Skinner MM, Richard L, et al. (2011) Methodological considerations for analyzing trabecular architecture: an example from the primate hand. *J Anat* **218**, 209–225.

Lovejoy CO (1975) Biomechanical perspectives on the lower limb of early hominids. In: *Primate Functional Morphology and Evolution*. (ed. Tuttle RH), pp. 291–326. The Hague: Mouton.

Lovejoy CO, McCollum MA (2010) Spinopelvic pathways to bipedality: why no hominids ever relied on a bent-hip–bent-knee gait. *Philos Trans R Soc Lond B Biol Sci* **365**, 3289–3299.

Lovejoy OC, Meindl RS, Ohman JC, et al. (2002) The Maka femur and its bearing on the antiquity of human walking: applying contemporary concepts of morphogenesis to the human fossil record. *Am J Phys Anthropol* **119**, 97–133.

MacLatchy L, Müller R (2002) A comparison of the femoral head and neck trabecular architecture of *Galago* and *Perodicticus* using micro-computed tomography (μCT). *J Hum Evol* **43**, 89–105.

Maga M, Kappelman J, Ryan TM, et al. (2006) Preliminary observations on the calcaneal trabecular microarchitecture of extant large-bodied hominoids. *Am J Phys Anthropol* **129**, 410–417.

Mann RA, Hagy J (1980) Biomechanics of walking running and sprinting. *Am J Sports Med* **8**, 345–350.

Maquer G, Musy SN, Wandel J, et al. (2015) Bone volume fraction and fabric anisotropy are better determinants of trabecular bone stiffness than other morphological variables. *J Bone Miner Res* **30**, 1000–1008.

McHenry HM, Corruccini RS (1978) The femur in early human evolution. *Am J Phys Anthropol* **49**, 473–487.

Milovanovic P, Danijela D, Michael H, et al. (2017) Region-dependent patterns of trabecular bone growth in the human proximal femur: a study of 3D bone microarchitecture from early postnatal to late childhood period. *Am J Phys Anthropol* **164**, 281–291.

Mittra E, Rubin C, Qin Y (2005) Interrelationship of trabecular mechanical and microstructural properties in sheep trabecular bone. *J Biomech* **38**, 1229–1237.

Miyakoshi N (2004) Effects of parathyroid hormone on cancellous bone mass and structure in osteoporosis. *Curr Pharm Des* **10**, 2615–2627.

Morbeck ME, Zihlman AL (1988) Body composition and limb proportions. In: *Orangutan Biology*. (ed. Schwartz JH), pp. 285–297. Oxford: Oxford University Press.

Myatt JP, Crompton RH, Thorpe SKS (2011) Hindlimb muscle architecture in non-human great apes and a comparison of methods for analysing inter-species variation. *J Anat* **219**, 150–166.

Myers CA, Register BC, Lertwanich P, et al. (2011) Role of the acetabular labrum and the iliofemoral ligament in hip stability: an *in vitro* biplane fluoroscopy study. *Am J Sports Med* **39**, 85–91.

Nakano Y, Hirasaki E, Kumakura H (2006) Patterns of vertical climbing in primates. In: *Human Origins and Environmental Backgrounds Developments in Primatology: Progress and Prospects*. (eds Ishida H, Tuttle R, Pickford M, Ogihara N, Nakatsukasa M), pp. 97–104. Boston: Springer.

Novacheck TF (1998) The biomechanics of running. *Gait Posture* **7**, 77–95.

Odgaard A (1997) Three-dimensional methods for quantification of cancellous bone architecture. *Bone* **20**, 315–328.

O'Neill MC, Lee L, Demes B, et al. (2015) Three-dimensional kinematics of the pelvis and hind limbs in chimpanzee (*Pan troglodytes*) and human bipedal walking. *J Hum Evol* **86**, 32–42.

Ounpuu S (1990) The biomechanics of running: a kinematic and kinetic analysis. *AAOS Instr Course Lect* **39**, 305–318.

Ounpuu S (1994) The biomechanics of walking and running. *Clin Sports Med* **13**, 843–863.

Paul JP (1976) Approaches to design – Force actions transmitted by joints in the human body. *Proc R Soc Lond B Biol Sci* **192**, 163–172.

Payne RC, Crompton RH, Isler K, et al. (2006) Morphological analysis of the hindlimb in apes and humans: II Moment arms. *J Anat* **208**, 725–742.

Pearson OM, Lieberman DE (2004) The aging of Wolff's 'law': ontogeny and responses to mechanical loading in cortical bone. *Am J Phys Anthropol* **125**, 63–99.

Pedersen DR, Brand RA, Davy DT (1997) Pelvic muscle and acetabular contact forces during gait. *J Biomech* **30**, 959–965.

Polk JD, Blumenfeld J, Ahlumwalia D (2008) Knee posture predicted subchondral apparent density in the distal femur: an experimental validation. *Anat Rec* **291**, 293–302.

Pontzer H, Lieberman DE, Momin E, et al. (2006) Trabecular bone in the bird knee responds with high sensitivity to changes in load orientation. *J Exp Biol* **209**, 57–65.

R Development Core Team (2017) *R: A Language and Environment for Statistical Computing*. Vienna: The R Foundation for Statistical Computing.

Rafferty KL (1998) Structural design of the femoral neck in primates. *J Hum Evol* **34**, 361–383.

Rafferty KL, Ruff CB (1994) Articular structure and function in *Hylobates, Colobus* and *Papio*. *Am J Phys Anthropol* **94**, 395–408.

Raichlen DA, Gordon AD, Harcourt-Smith WEH, et al. (2010) Laetoli footprints preserve earliest direct evidence of human-like bipedal biomechanics. *PLoS One* **5**, e9769.

Reissis D, Abel RL (2012) Development of fetal trabecular microarchitecture in the humerus and femur. *J Anat* **220**, 496–503.

Remis MJ (1995) Effects of body size and social context on the arboreal activities of lowland gorillas in the Central African Republic. *Am J Phys Anthropol* **97**, 413–433.

Remis MJ (1999) Tree structure and sex differences in arboreality among western lowland gorillas (*Gorilla gorilla gorilla*) at Bai Hokou Central African Republic. *Primates* **40**, 383.

Rodan GA (1998) Bone homeostasis. *Proc Natl Acad Sci U S A* **95**, 13361–13362.

Rubin CT, McLeod KJ, Bain SD (1990) Functional strains and cortical bone adaptation: epigenetic assurance of skeletal integrity. *J Biomech* **23**, 43–49.

Rubin CT, Turner AS, Bain S, et al. (2001) Low mechanical signals strengthen long bones. *Nature* **412**, 603.

Ruff CB (1995) Biomechanics of the hip and birth in early Homo. *Am J Phys Anthropol* **98**, 527–574.

Ruff CB (2002) Long bone articular and diaphyseal structure in old world monkeys and apes I: locomotor effects. *Am J Phys Anthropol* **119**, 305–342.

Ruff CB, Higgins R (2013) Femoral neck structure and function in early hominins. *Am J Phys Anthropol* **150**, 512–525.

Ruff CB, Runestad JA (1992) Primate limb bone structural adaptations. *Annu Rev Anthropol* **21**, 407–433.

Ruff CB, Scott WW, Liu AY-C (1991) Articular and diaphyseal remodeling of the proximal femur with changes in body mass in adults. *Am J Phys Anthropol* **86**, 397–413.

Ryan TM, Ketcham RA (2002) The three-dimensional structure of trabecular bone in the femoral head of strepsirrhine primates. *J Hum Evol* **43**, 1–26.

Ryan TM, Ketcham RA (2005) Angular orientation of trabecular bone in the femoral head and its relationship to hip joint loads in leaping primates. *J Morphol* **265**, 249–263.

Ryan TM, Krovitz GE (2006) Trabecular bone ontogeny in the human proximal femur. *J Hum Evol* **51**, 591–602.

Ryan TM, Shaw CN (2012) Unique suites of trabecular bone features characterize locomotor behavior in human and non-human anthropoid primates. *PLoS One* **7**, e41037.

Ryan TM, Shaw CN (2013) Trabecular bone microstructure scales allometrically in the primate humerus and femur. *Proc Biol Sci* **280**, 20130172.

Ryan TM, Shaw CN (2015) Gracility of the modern *Homo sapiens* skeleton is the result of decreased biomechanical loading. *Proc Natl Acad Sci U S A* **112**, 372–377.

Ryan TM, Walker A (2010) Trabecular bone structure in the humeral and femoral heads of anthropoid primates. *Anat Rec (Hoboken)* **293**, 719–729.

Ryan TM, Carlson KJ, Gordon AD, et al. (2018) Hyman-like hip joint loading in *Australopithecus africanus* and *Paranthropus robustus*. *J Hum Evol* **121**, 12–24.

Saers JPP, Cazorla-Bak Y, Shaw CN, et al. (2016) Trabecular bone structural variation throughout the human lower limb. *J Hum Evol* **97**, 97–108.

San Millán M, Kaliontzopoulou A, Rissech C, et al. (2015) A geometric morphometric analysis of acetabular shape of the primate hip joint in relation to locomotor behaviour. *J Hum Evol* **83**, 15–27.

Scherf H (2008) Locomotion-related femoral trabecular architectures in primates — high resolution computed tomographies and their implications for estimations of locomotor preferences of fossil primates. In: *Anatomical Imaging: Towards a New Morphology*. (eds Endo H, Frey R), pp. 39–59. Tokyo: Springer Japan.

Scherf H, Tilgner R (2009) A new high-resolution computed tomography (CT) segmentation method for trabecular bone architectural analysis. *Am J Phys Anthropol* **140**, 39–51.

Scherf H, Harvati K, Hublin J-J (2013) A comparison of proximal humeral cancellous bone of great apes and humans. *J Hum Evol* **65**, 29–38.

Schneider CA, Rasband WS, Eliceiri KW (2012) NIH Image to ImageJ: 25 years of image analysis. *Nat Methods* **9**, 671–675.

Schultz AH (1969) Observations on the acetabulum of primates. *Folia Primatol* **11**, 181–199.

Shaw CN, Ryan TM (2012) Does skeletal anatomy reflect adaptation to locomotor patterns? Cortical and trabecular architecture in human and nonhuman anthropoids. *Am J Phys Anthropol* **147**, 187–200.

Simkin A, Ayalon J, Leichter I (1987) Increased trabecular bone density due to bone-loading exercises in postmenopausal osteoporotic women. *Calcif Tissue Int* **40**, 59–63.

Skinner MM, Stephens NB, Tsegai ZJ, et al. (2015) Human-like hand use in *Australopithecus africanus*. *Science* **347**, 395–399.

Slocum DB, James SL (1968) Biomechanics of running. *JAMA* **205**, 721–728.

Smith DM, Nance WE, Kang KW, et al. (1973) Genetic factors in determining bone mass. *J Clin Investig* **52**, 2800–2808.

Sonntag CF (1923) On the anatomy physiology and pathology of the chimpanzee. *Proc Zool Soc Lond* **93**, 323–429.

Sonntag CF (1924) On the anatomy physiology and pathology of the Orang-Outan (17). *Proc Zool Soc Lond* **94**, 349–450.

Stauber M, Rapillard L, van Lenthe GH, et al. (2006) Importance of individual rods and plates in the assessment of bone quality and their contribution to bone stiffness. *J Bone Mine Res* **21**, 586–595.

Stephens NB, Kivell TL, Thomas G, et al. (2016) Trabecular architecture in the thumb of *Pan* and *Homo*: implications for investigating hand use loading and hand preference in the fossil record. *Am J Phys Anthropol* **161**, 603–619.

Stern JT Jr, Susman RL (1983) The locomotor anatomy of *Australopithecus afarensis*. *Am J Phys Anthropol* **60**, 279–317.

Sugardjito J, van Hooff JARAM (1986) Age-sex class differences in the positional behaviour of the Sumatran Orang-Utan (*Pongo pygmaeus abelii*) in the Gunung Leuser National Park Indonesia. *Folia Primatol* **47**, 14–25.

Susman RL, Stern JJT, Jungers WL (1984) Arboreality and bipedality in the hadar hominids. *Folia Primatol* **43**, 113–156.

Suuriniemi M, Anitta M, Vuokko K, et al. (2004) Association between exercise and pubertal BMD is modulated by estrogen receptor α genotype. *J Bone Miner Res* **19**, 1758–1765.

Sylvester AD, Terhune CE (2017) Trabecular mapping: leveraging geometric morphometrics for analyses of trabecular structure. *Am J Phys Anthropol* **163**, 553–569.

Thomason JJ (1985a) Estimation of locomotory forces and stresses in the limb bones of Recent and extinct equids. *Paleobiology* **11**, 209–220.

Thomason JJ (1985b) The relationship of trabecular architecture to inferred loading patterns in the third metacarpals of the extinct equids Merychippus and Mesohippus. *Paleobiology* **11**, 323–335.

Thorpe SKS, Crompton RH (2005) Locomotor ecology of wild orangutans (*Pongo pygmaeus abelii*) in the Gunung Leuser Ecosystem Sumatra Indonesia: a multivariate analysis using log-linear modelling. *Am J Phys Anthropol* **127**, 58–78.

Thorpe SKS, Crompton RH (2006) Orangutan positional behavior and the nature of arboreal locomotion in Hominoidea. *Am J Phys Anthropol* **131**, 384–401.

Thorpe SKS, Holder R, Crompton RH (2009) Orangutans employ unique strategies to control branch flexibility. *Proc Natl Acad Sci U S A* **106**, 12646–12651.

Treece GM, Gee AH (2014) Independent measurement of femoral cortical thickness and cortical bone density using clinical CT. *Med Image Anal* **20**, 249–264.

Tsegai ZJ, Kivell TL, Gross T, et al. (2013) Trabecular bone structure correlates with hand posture and use in hominoids. *PLoS One* **8**, e78781.

Tsegai ZJ, Skinner MM, Gee AH, et al. (2017) Trabecular and cortical bone structure of the talus and distal tibia in *Pan* and *Homo*. *Am J Phys Anthropol* **163**, 784–805.

Tsegai ZJ, Skinner MM, Pahr DH, et al. (2018) Systemic patterns of trabecular bone across the human and chimpanzee skeleton. *J Anat* **232**, 641–656.

Tuttle RH, Cortright W (1988) Positional behavior adaptive complexes and evolution. In: *Orangutan Biology*. (ed. Schwartz JH), pp. 311–330. Oxford: Oxford University Press.

Van der Bogert AJ, Read L, Nigg BM (1999) An analysis of hip joint loading during walking running and skiing. *Med Sci Sports Exerc* **31**, 131–142.

Volpato V, Viola TB, Nakatsukasa M, et al. (2008) Textural characteristics of the iliac-femoral trabecular pattern in a bipedally trained Japanese macaque. *Primates* **49**, 16–25.

Wagner FV, Negrão JR, Campos J, et al. (2012) Capsular ligaments of the hip: anatomic histologic and positional study in Cadaveric Specimens with MR Arthrography. *Radiology* **263**, 189–198.

Wallace IJ, Demes B, Mongle C, et al. (2014) Exercise-induced bone formation is poorly linked to local strain magnitude in the sheep tibia. *PLoS One* **9**, e99108.

Wallace IJ, Demes B, Judex S (2017) Ontogenetic and genetic influences on bone's responsiveness to mechanical signals. In: *Building Bones: Bone Formation and Development in Anthropology*. (eds Percival CJ, Richtsmeier JT), pp. 233–253. Cambridge: Cambridge University Press.

Walsh JS (2015) Normal bone physiology remodelling and its hormonal regulation. *Surgery (Oxford)* **33**, 1–6.

Ward FO (1838) *Outlines of Human Osteology*. London: Henry Renshaw.

Ward CV (1991) Functional anatomy of the lower back and pelvis of the Miocene hominoid *Proconsul nyanzae* from Mfanga Island Kenya. PhD Dissertation, Johns Hopkins University.

Ward CV (2002) Interpreting the posture and locomotion of *Australopithecus afarensis*: where do we stand? *Am J Phys Anthropol* **119**, 185–215.

Whalen RT, Carter DR, Steele CR (1988) Influence of physical activity on the regulation of bone density. *J Biomech* **21**, 825–837.

Whitehouse WJ (1974) The quantitative morphology of anisotropic trabecular bone. *J Microsc* **101**, 153–168.

Wolff J (1892) *Das Gesetz der Transformation der Knochen*. Berlin: A Hirchwild.

Wolff J (1870) Uber die innere Architektur der Knochen und ihre bedeutung fur die Frage vom Knochenwachstum. *Virchows Archiv fur Pathologische Anatomie und Physiologie* **50**, 389–453.

Yoshida H, Faust A, Wilckens J, et al. (2006) Three-dimensional dynamic hip contact area and pressure distribution during activities of daily living. *J Biomech* **39**, 1996–2004.